NASA Technical Memorandum 107461
ASME–97–GT–439

Mixing of Multiple Jets With a Confined Subsonic Crossflow

Part II—Opposed Rows of Orifices in Rectangular Ducts

James D. Holdeman
Lewis Research Center
Cleveland, Ohio

David S. Liscinsky
United Technologies Research Center
East Hartford, Connecticut

Daniel B. Bain
CFD Research Corporation
Huntsville, Alabama

Prepared for the
42nd Gas Turbine and Aeroengine Congress
sponsored by the International Gas Turbine Institute of
the American Society of Mechanical Engineers
Orlando, Florida, June 2–5, 1997

National Aeronautics and
Space Administration

Mixing of Multiple Jets With a Confined Subsonic Crossflow Part II - Opposed Rows of Orifices in Rectangular Ducts

James D. Holdeman*
NASA Lewis Research Center
Cleveland, OH 44135

David S. Liscinsky+**
United Technologies Research Center
E. Hartford, CT 06108

Daniel B. Bain**
CFD Research Corporation
Huntsville, AL 35805

Abstract

This paper summarizes experimental and computational results on the mixing of opposed rows of jets with a confined subsonic crossflow in rectangular ducts. The studies from which these results were excerpted investigated flow and geometric variations typical of the complex 3-D flowfield in the combustion chambers in gas turbine engines.

The principal observation was that the momentum-flux ratio, J, and the orifice spacing, S/H, were the most significant flow and geometric variables. Jet penetration was critical, and penetration decreased as either momentum-flux ratio or orifice spacing decreased. It also appeared that jet penetration remained similar with variations in orifice size, shape, spacing, and momentum-flux ratio when the orifice spacing was inversely proportional to the square-root of the momentum-flux ratio. It was also seen that planar averages must be considered in context with the distributions. Note also that the mass-flow ratios and the orifices investigated were often very large (jet-to-mainstream mass-flow ratio >1 and the ratio of orifices-area-to-mainstream-cross-sectional-area up to 0.5 respectively), and the axial planes of interest were often just downstream of the orifice trailing edge. Three-dimensional flow was a key part of efficient mixing and was observed for all configurations.

Nomenclature

A_j/A_m = jet-to-mainstream area ratio
AC_d = $(A_j)(C_d)$
B = orifice blockage
C = $(S/H)\sqrt{J}$
C_{avg} = equilibrium concentration
= θ_{EB}
C_d = orifice discharge coefficient
C_i = local concentration
d = orifice diameter
DR = jet-to-mainstream density ratio
H = duct height
J = jet-to-mainstream momentum-flux ratio
= $(DR)(V_j/U_m)^2$
= $(MR)^2/((DR)(C_d)^2(A_j/A_m)^2)$
L = long dimension of orifice
L/W = orifice aspect ratio
m = number of pixels in the distribution
MR = jet-to-mainstream mass-flow ratio
= w_j/w_m
= $(\sqrt{DR})(\sqrt{J})(C_d)(A_j/A_m)$
S = lateral spacing between corresponding parts of adjacent orifices
T = temperature
T_j = jet exit temperature
T_m = mainstream temperature
θ = $(T_m - T)/(T_m - T_j)$
U_m = mainstream velocity
U_s = spatial unmixedness
V_j = jet velocity
w_j/w_T = jet-to-total mass-flow ratio
= MR/(MR + 1)
W = short dimension of orifice
x = downstream coordinate
= 0 at leading edge of orifice
y = cross-stream coordinate
= 0 at wall
z = lateral coordinate
= 0 at centerplane

---

* Senior Research Engineer
\+ Research Scientist
** Research Engineer

1. Introduction

Jets-in-crossflow have been extensively treated in the literature. Flows in which this is an integral constituent occur in a number of areas important in combustion and energy science and technology. In a gas turbine combustor for example, fuel and air mixing is important to combustor performance and emissions. Also, the mixing associated with arrays of jets in crossflow can play a critical role as in the dilution zone of a conventional combustor, and the mixing zone of a staged combustor such as the Rich-burn/Quick-mix/Lean-burn (RQL) combustor. Although results reported to date have all contributed additional understanding of the general problem, the information obtained in them was determined by their motivating application, and may not satisfy the specific needs of different applications.

One characteristic of jet-in-crossflow applications in gas turbine combustion chambers is that they are often confined mixing problems, with up to 80 percent of the total flow entering through the jets. The result is that the equilibrium mixing pattern and composition of the exiting flow may differ significantly from that of the entering mainstream flow.

A summary of NASA-supported research in the 1980's is given in Holdeman (1993). Reports and papers from NASA-supported studies in a cylindrical duct that were published since the previous article was presented are summarized by Holdeman et al. (1996). Recent results from rectangular and annular configurations include, Bain et al. (1992-1995b), Bain et al. (1996), Blomeyer et al. (1996), Chiu, Roth, Margason & Tso (1993), Chiu, Roth, Karlin, Margason & Tso (1993), Crocker & Smith (1992 & 1993), Crocker et al. (1994), Doerr & Henneke (1993), Doerr et al. (1995a & 1995b), Everson et al. (1995), Liscinsky et al. (1992), Liscinsky, Vranos, & Lohmann (1993), Liscinsky, True, & Holdeman (1993), Liscinsky et al. (1994-1996b), Lozano et al. (1991), Lozano et al. (1992), Margason (1993), Margason & Tso (1993), Mungal et al. (1992), Nikjooy et al. (1993), Smith et al. (1992), and Winter et al. (1992).

2. Description of the Flowfield

Figure 1 shows a schematic of the flow in a rectangular duct with injection from opposed rows of jets on top and bottom walls. The scalar field results are often presented as plots of the temperature difference ratio, θ, where

$$\theta = \frac{(T_m - T)}{(T_m - T_j)}$$

or,

$$1 - \theta = \frac{(T - T_j)}{(T_m - T_j)} \qquad (1)$$

It should be noted that although T is used here, these parameters can be defined with concentrations or any conserved scalar. Also note that the jet fluid is identified by larger values of θ (i.e. $\theta = 0$ if $T = T_m$) and $\theta = 1$ if $T = T_j$. Unless noted otherwise, jet fluid will be colored white, and mainstream fluid will be colored black. The equilibrium jet mass fraction for any configuration is approximately equal to the fraction of the total flow entering through the jets, MR/(MR + 1).

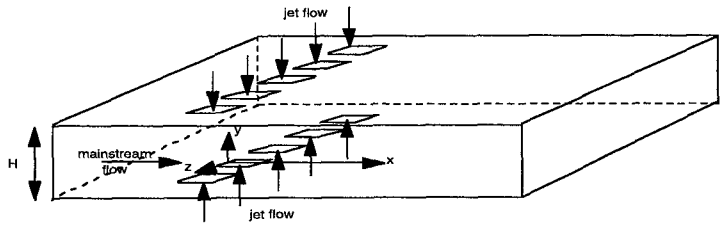

Figure 1: Schematic of Numerical Mixing Model (from Bain et al. (1995b))

If one averages a conserved scalar across a y-z plane downstream of the orifice trailing edge, the result is herein called C_{avg}. It has been shown by Liscinsky et al. (1993) that this value is nearly equal to the value of a fully mixed flow. Another planar averaged parameter is the variance, often called spatial unmixedness (in this paper unmixedness = spatial unmixedness). Note that this variance has been normalized by dividing by the product of C_{avg} and $(1-C_{avg})$.

$$U_s = \frac{\frac{1}{m}\sum_{i=1}^{m}(C_i - C_{avg})^2}{C_{avg}(1 - C_{avg})} \qquad (2)$$

Although it is recognized that a uniform distribution may not always be desired, optimum is generally used herein (as in e.g. Holdeman 1993) to identify flow and geometric conditions which lead to a uniform distribution in a minimum downstream distance. The primary independent geometric variables are the spacing between adjacent orifices, S, the orifice diameter, d; the orifice aspect ratio (long:short dimension), and the slant angle (with respect to the axial direction in the plane of the orifice). Because the objective in combustor applications is to identify configurations that provide a desired mixing pattern within a given downstream distance, locations of interest are identified in intervals of the duct height, H, rather than the orifice diameter, d. The primary independent flow variables are the jet-to-mainstream mass-flow ($MR = w_j/w_m$) and momentum-flux (J) ratios. These can be expressed as:

$$J = \frac{MR^2}{(DR)(C_d)^2(A_j/A_m)^2} \qquad (3)$$

It was reported in Holdeman (1993) that jet penetration and centerplane profiles appear to be similar when the orifice spacing and the square root of the momentum-flux ratio were inversely proportional, i.e.:

$$C = (S/H)\sqrt{J} \qquad (4)$$

For single-side injection (& with $MR < .5$), the centerplane profiles were approximately centered across the duct height and approached an isothermal distribution in the minimum downstream distance when $C = 2.5$. This appeared to be independent of orifice diameter, as shown in both calculated and experimental profiles. The similarity of the profiles with the same orifice spacing but with different orifice diameters were also shown by Holdeman et al. (1973). Values of C in Eq. 4 which were a factor of 2 or more smaller or larger than the optimum corresponded to gross underpenetration or overpenetration respectively. For opposed rows of in-line orifices, the optimum C was approximately half of the corresponding value for single-side injection; whereas for opposed rows of staggered orifices, the optimum C was approximately doubled.

It has been recognized that what configuration is deemed "optimum" depend on the downstream location examined, so C in Eq. 4 must be a function of x/H. It has also been shown in recent studies of rectangular duct flows that C may be a function of something else too, e.g. for high mass-flow ratios the optimum C appeared to be about twice that found previously. Note that although the proportionality in Eq. 4 appears to hold for all cases, the value of the constant may vary with duct geometry, orifice shape, initial conditions and mass-flow ratio.

3. Results and Discussion

The following paragraphs describe the results from recent investigations in the context of the effects of the primary independent variables. Both experimental and computational studies were performed, and are interspersed here. The work cited was performed by CFD Research Corporation, and the United Technologies Research Center. Sources are identified when results are discussed, and specifics of the calculations or experiments, as appropriate, are given in the corresponding references. Note also that the original figures often appear in color in the references.

In Figure 1, x is the downstream coordinate, with x=0 at the leading edge of the orifices. Sharp-edged orifices were considered in all cases. In the experiments, discharge coefficients were measured in separate experiments. The orifice area, A_j, was a physical dimension, so the effective area, AC_d, was $((C_d)(A_j))$. For all calculations shown herein, a uniform flow boundary was assumed for both the jets and mainstream. Since the orifice discharge coefficient, C_d, was expected to be less than unity for the jets, the area over which the uniform velocity was specified was the effective area. A_j could thus be determined as needed from the AC_d by assuming an effective discharage coefficient.

Investigations published prior to 1991 were primarily in a rectangular duct, but at significantly lower mass-flow ratios than in more recent studies. A schematic showing the relative orifice size is given in Figure 2. Effects investigated were: 1) variation of momentum-flux ratio (J) at constant orifice shape and spacing; 2) variation of orifice spacing, S/H, at constant J; 3) effect of orifice shape; 4) comparison of slanted slots & holes; 5) comparison of an opposed row of in-line and staggered jets; 6) effects of non-symmetric mass addition; 7) effect of orifice blockage; and 8) variation of mass-flow ratio. These are discussed in the following sections.

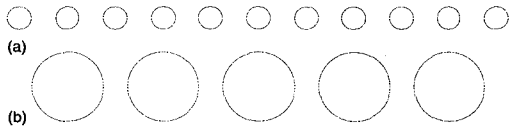

Figure 2: Example orifice geometry - (a) previous dilution jet mixing, (b) current investigations (from Holdeman et al. 1996)

3.1 Variation of momentum-flux ratio

Based on previous studies which reported that the most important flow variable influencing the extent of jet mixing in a crossflow was the momentum-flux ratio, J, Liscinsky et al. (1992) performed a series of tests with S/H = 0.5 at two representative J values. The results reaffirmed the importance of the momentum-flux ratio in determining the downstream flowfield.

Jet penetration generally increases with increasing momentum-flux ratio, J. This can be seen in the experimental results for both slanted slots and round holes reported by Liscinsky et al (1992). A similar effect is apparent in the calculated results of Bain et al. (1993) for a configuration with aligned slots of 4:1 aspect ratios at S/H = 0.325.

The planar unmixedness for both the Liscinsky et al. (1992) and Bain et al. (1994) cases suggest that it is possible to obtain low values of unmixedness at J values corresponding to overpenetration. This emphasizes that although planar averaged values are very useful and can provide insight, one should not rely on them alone, and must also assess the flowfield distributions.

3.2 Variation of orifice spacing

In general, the effect of decreasing the orifice spacing at constant J is similar to the effect of decreasing the momentum-flux ratio at constant S/H. This effect was shown in the computational study by Bain et al. (1993).

Figure 3 shows isotherms of the centerplane (vertical-axial plane through the geometric center of the orifice) for different spacings of 4:1 aligned slots for J=36. The jet penetration increases as the spacing increases. At the smaller S/H the jets underpenetrate, allowing the approach flow to pass through the center of the duct. As S/H increases, the jets penetrate farther, beginning to pinch off the approach flow along the duct centerplane. At larger spacing, the jets have clearly overpenetrated, blocking off the approach flow near the center and forcing more of the mainstream flow adjacent to the walls and between the jets.

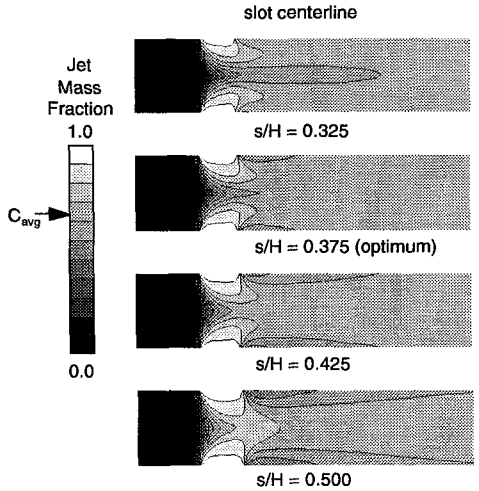

Figure 3: Effect of varying jet spacing on calculated jet distibutions for inline slots; J = 36, MR = 2.0 (data from Bain et al. (1995b))

The optimum mixer appears to be at about S/H = 0.375 for J = 36, which agrees well with the optimum S/H that would be identified from the unmixedness plots in Figure 4.

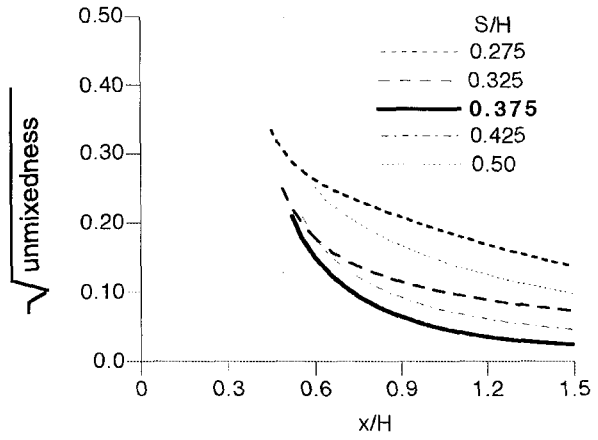

Figure 4: Effect of varying jet spacing on unmixedness; J = 36 (data from Bain et al. (1995b))

A similar effect is apparent in the experimental results of Liscinsky et al. (1993). Mean concentration distributions for opposed rows of round holes with centerlines opposite each other is shown in Figure 5 for J = 25 at x/H = 0.375 and x/H = 0.5. In each column S/H decreases from 0.75 at the top to 0.4 at the bottom. The effect of the confinement is apparent, as these distributions show overpenetration at the largest spacing, and underpenetration at the smaller, with the "optimum" spacing depending on the axial distance of interest.

The corresponding unmixedness plots are shown in Figure 6. S/H = 0.5 appears to be the best mixer, which is consistent with the configuration one would pick from Figure 5.

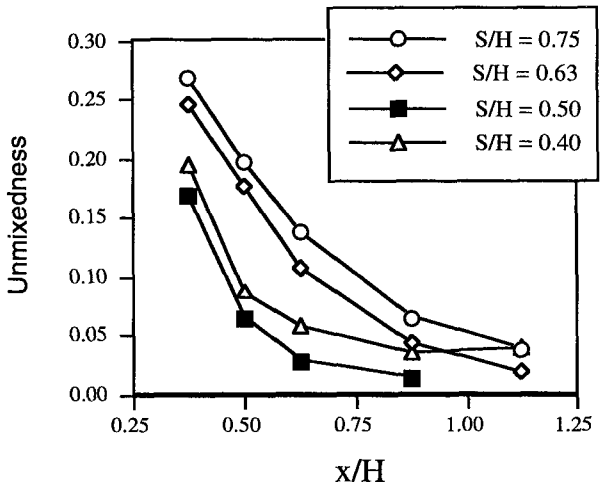

Figure 6: Effect of orifice spacing on spatial unmixedness for inline round holes; H/d = 2.67, J = 25 (data from Liscinsky et al. (1993))

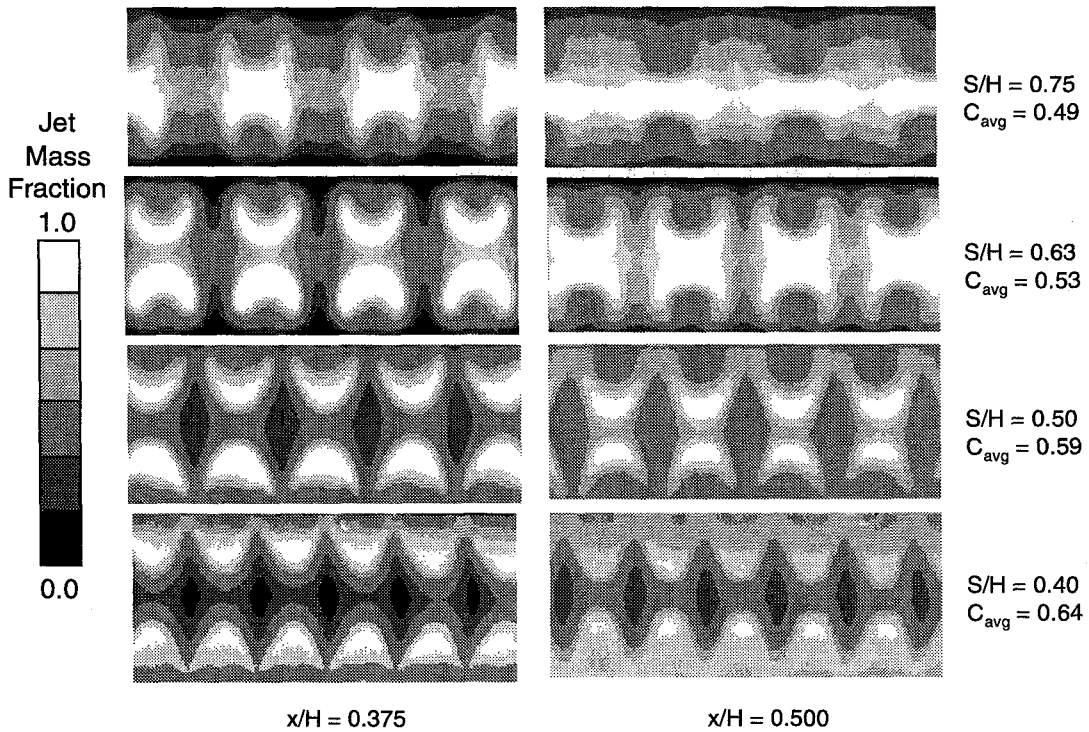

Figure 5: Average concentration distributions for opposed inline round holes; H/d = 2.67, J = 25 (data from Liscinsky et al. (1993))

3.3 Effects of orifice shape

The orifice shape changes the jet surface area and also affects 1) the amount of jet mass injected per unit length, and 2) the axial domain over which the mass is injected. Generally, increasing the ratio of the long to short dimension of low aspect ratio aligned slots has little effect on jet penetration. This is seen in Figures 7 and 8 from the computational results reported by Bain et al. (1994). The planes shown in Figure 7 are vertical-axial ones through the orifice centers, with the corresponding vertical-transverse planes at x/H = 0.5 shown in Figure 8. For each case, the jets penetrate approximately one quarter of the duct height, although there are some subtle differences between these shapes. The most recognizable of these being the difference between the square and the other orifice shapes, as the jets from the square orifice appear to penetrate slightly less as shown by less mainstream fluid in the wake of the injection for the square.

Perhaps this slight effect is related to the wake width of these orifices. Figure 9 shows velocity vectors in a transverse-axial plane next to the wall. Near the wall the jets act as a bluff body to the mainstream flow. This flow then accelerates around the jet prior to separating and forming a wake. As the base area increases, the width of this region increases. Although at its diameter the circle is wider than the square, the width of the wake is less for the round hole as the approach flow remains attached beyond its maximum width. Thus, the square has the widest wake and it follows that its penetration is slightly less.

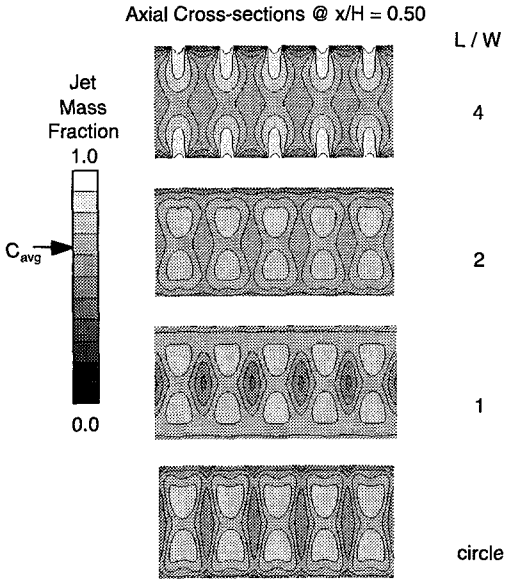

Figure 8: Effect of orifice aspect ratio on jet penetration; J = 36, MR = 2.0 (data from Bain et al. (1994))

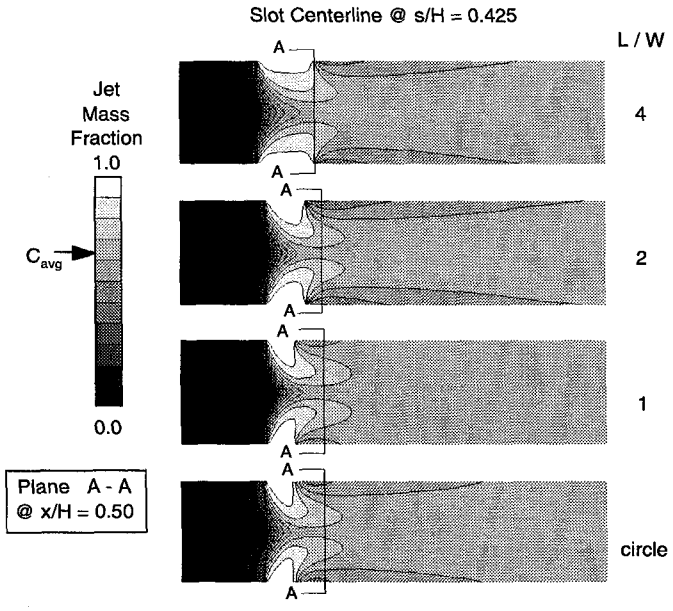

Figure 7: Effect of orifice aspect ratio on jet penetration; J = 36, MR = 2.0 (data from Bain et al. (1994))

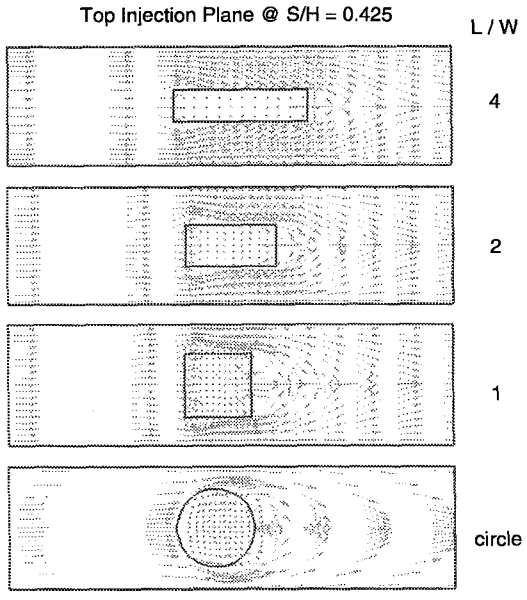

Figure 9: Effect of orifice aspect ratio on jet wakes; J = 36, MR = 2.0 (data from Bain et al. (1994))

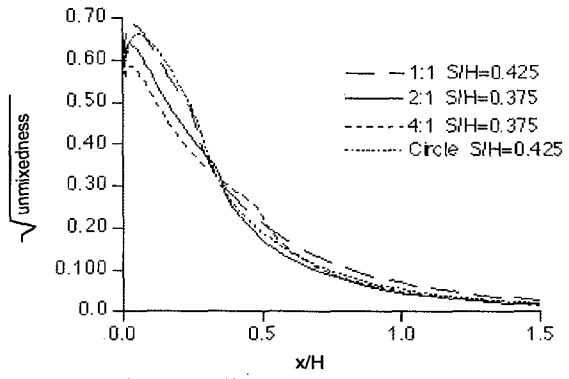

Figure 10: Effect of orifice aspect ratio on unmixedness; J = 36, MR = 2.0 (data from Bain et al. (1994))

The effect of orifice shape on unmixedness is illustrated in Figure 10. These curves are all presented at the optimum spacing for each configuration. In the near orifice region there are sizable differences between these, but aft of the orifice trailing edge all configurations essentially yield the same level of unmixedness.

The effect of orifice shape can also be seen experimentally in the results of Liscinsky et al. (1994). In Figure 11 average jet mass fraction concentration distributions are shown for square, circle, and 2D slot configurations. The concentration distributions downstream of the 2D slot indicates that the mainstream fluid remains near the center of the duct while the jet fluid stays near the walls. The mixing in this case appears slower than that for either the square or circular orifices. At x/H = 0.5 the distributions for the latter two configurations appear quite similar.

The corresponding unmixedness for these configurations is shown in Figure 12. These results confirm the observations above in that there is very little difference between the circle and square, and the unmixedness for the 2D slot is larger than both at all downstream distances.

The data in Figures 11 & 12 are consistent with the single jet results in Liscinsky et al. (1995, 1996) which also show little effect of orifice shape on the mean trajectory and mixing.

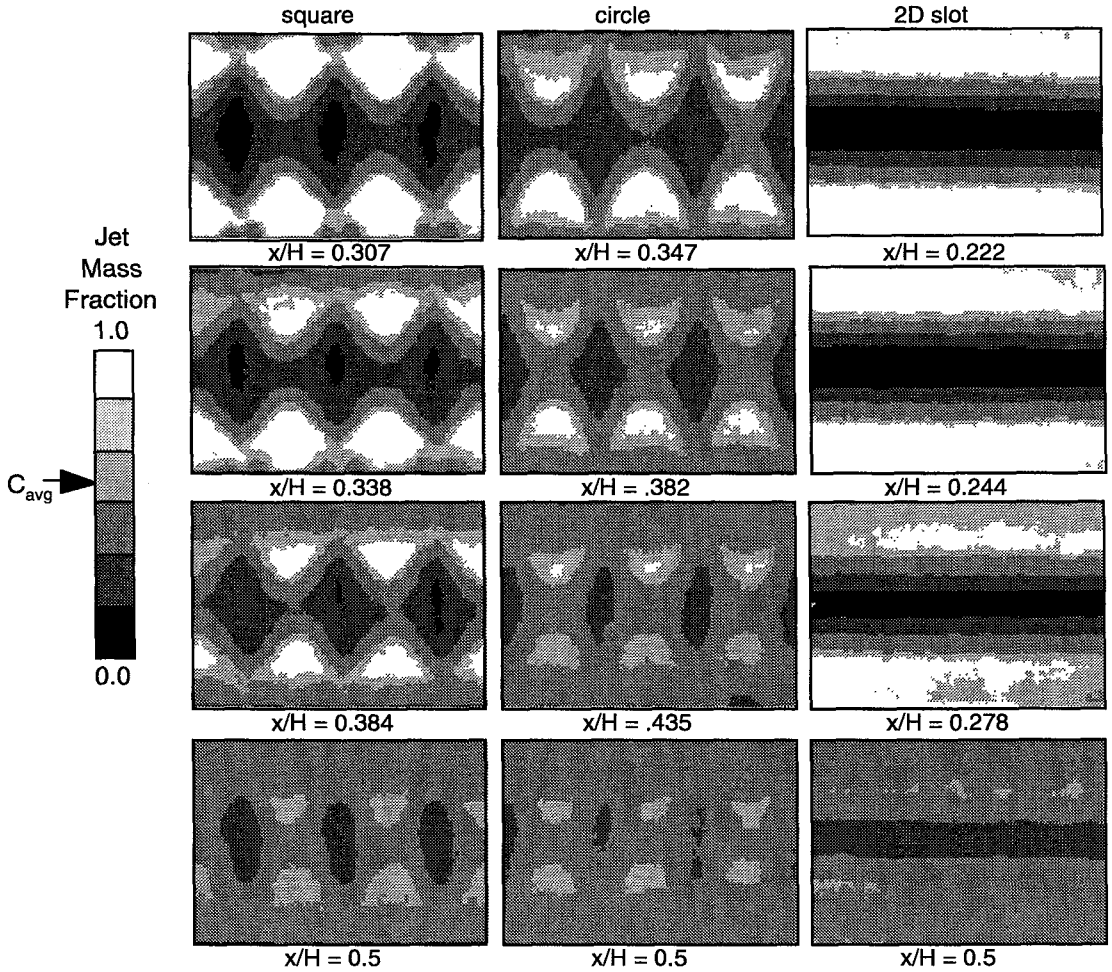

Figure 11: Effect of Orifice Shape on Opposed Inline Orifices; J = 48, MR = 2.0, S/H = 0.425 (data from Liscinsky et al. (1994))

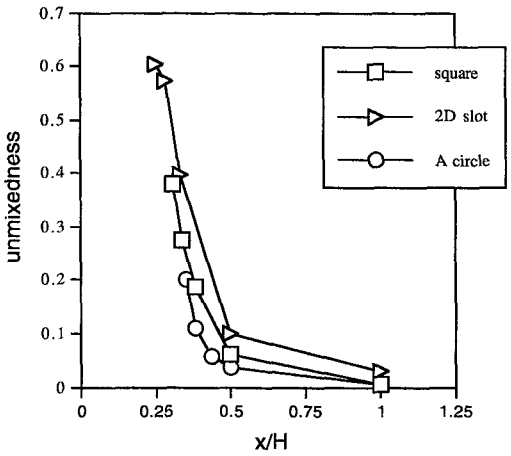

Figure 12: Effect of orifice shape on unmixedness; J = 48, MR = 2.0, S/H = 0.425 (data from Liscinsky et al. (1994))

3.4 Comparison of slanted slots and holes

Crossflow jet mixing performance is directly related to jet penetration, with optimum mixing for in-line configurations occurring when the asymptotic trajectory is near H/4. Previous studies (e.g. Hatch et al., 1995 & Oechsle et al., 1992) showed that jet trajectory varied with orifice slant angle. Therefore, in addition to orifice spacing, slot angle can be used to modify jet penetration. The characteristics of aligned opposed rows of round holes and 45 deg slanted slots of 4:1 aspect ratio were investigated by Liscinsky et al. (1994).

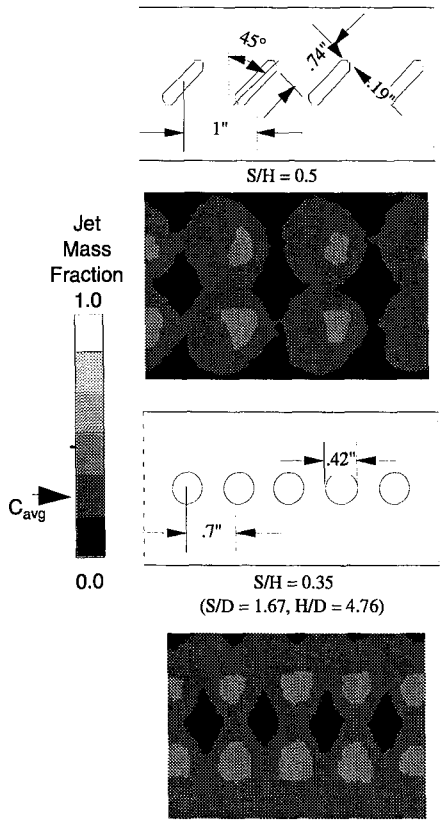

Figure 13: Orifice configurations and concentration distributions for 45 deg 4:1 slots and round holes; x/H = 0.5 and J = 25 (data from Liscinsky et al. (1994))

Drawings of the two configurations and their corresponding concentration distributions at x/H = 0.5 are shown in Figure 13. Each orifice is equal in area, however the round hole spacing was decreased to reduce jet penetration so it was equal to that for the slanted slots. Also, the gross mixing is similar for the two systems. Although the orifice shape modifies the jet concentration distribution in the vicinity of the orifice, downstream mixing appears to be independent of shape for slanted slot and round holes, when aerodynamic equivalent cases are compared.

Another experimental comparison of slanted slots and round holes is shown in Liscinsky et al. (1992). The distributions for slanted slots are given in Figure 14 as a function of downstream distance at momentum-flux ratios (J) of 16 and 36.

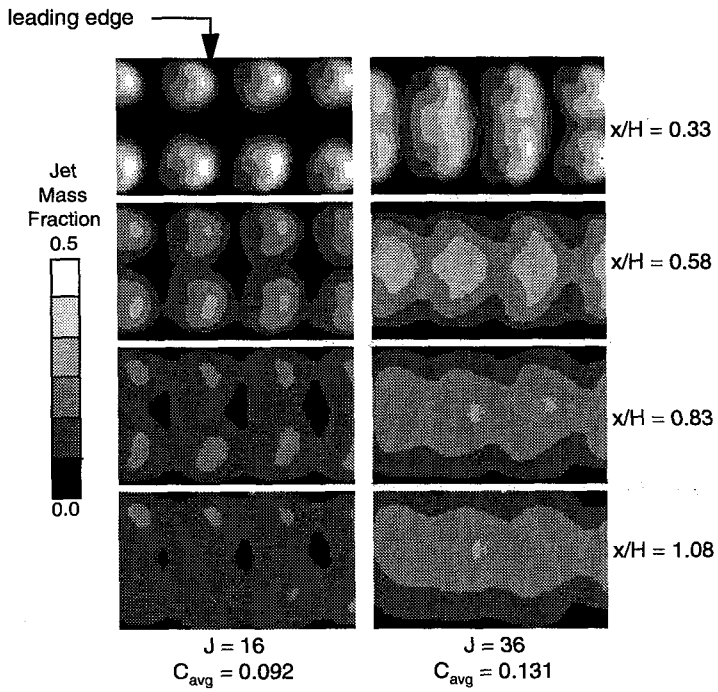

Figure 14: Effect of momentum-flux ratio and downstream distance on the average concentration distributions of the flow through opposed inline 45 deg slanted slots (data from Liscinsky et al. (1992))

The top and bottom slots slant in the same direction. In this configuration, the slanted slot jet forms a pair of counter-rotating vortices that are of unequal size and strength. The vortex formed at the leading edge of the orifice is larger and stronger than that formed at the trailing edge. The pair rotates so that the bulk of the jet fluid is toward the side that is upstream, thereby identifying the direction that the slot is slanted (in Fig.14 the upstream edge of the slot is on the right).

The corresponding distributions for circular holes are shown in Figure 15. It is obvious the vortex structure is different, and that the circular holes penetrate farther into the mainstream at each distance for each J.

The unmixedness curves are shown in Figure 16 and confirm the previous observation that there is little difference in gross mixing between slanted slots and round holes although differences in this parameter might be expected given the difference observed in the vortex structure.

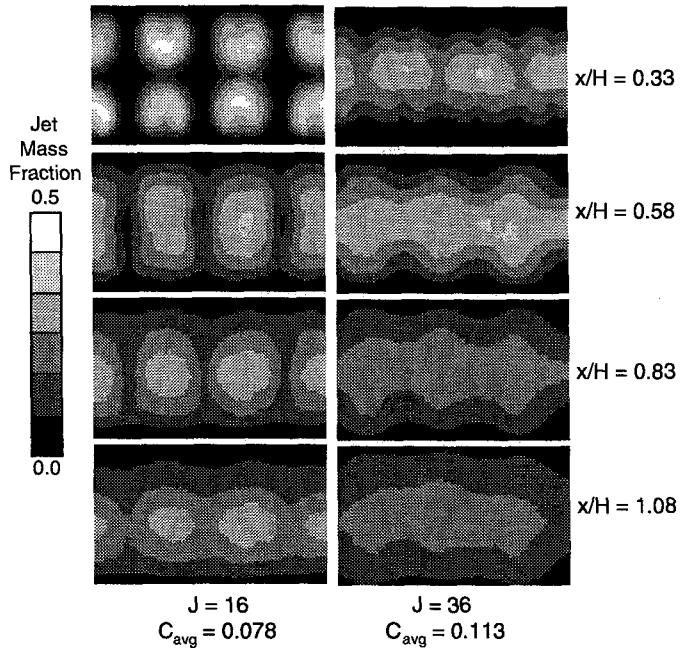

Figure 15: Effect of momentum-flux ratio and downstream distance on the average concentration distributions of the flow through opposed inline round holes (data from Liscinsky et al. (1994))

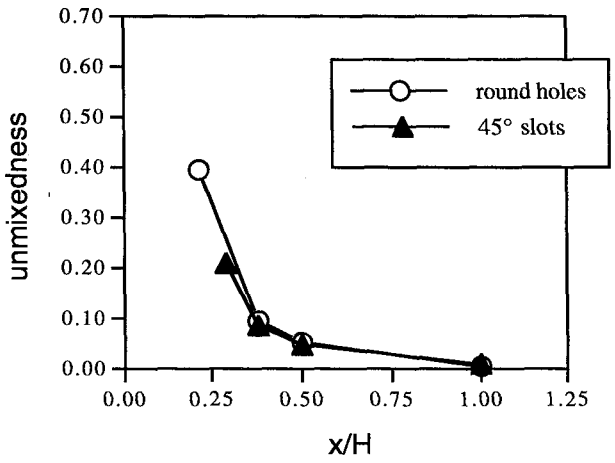

Figure 16: Comparison of spatial unmixedness for equivalent 45 deg slot and round hole configurations at J = 25 (data from Liscinsky et al. 1994)

3.5 Comparison of an opposed row of in-line and staggered jets

The effect of lateral arrangement is shown in the results of Bain et al. (1995b). Unmixedness curves for J = 16, 36, and 64 are given in Figures 17, 18, and 19 respectively, where only the curves corresponding to optimum spacing are shown. In each figure, it is apparent that in-line configurations gave better initial mixing, probably due to their significantly smaller size. Farther downstream (e.g. at x/H = 1) in-line configurations appear better at J = 16, but staggered arrangements show better mixing at J = 64.

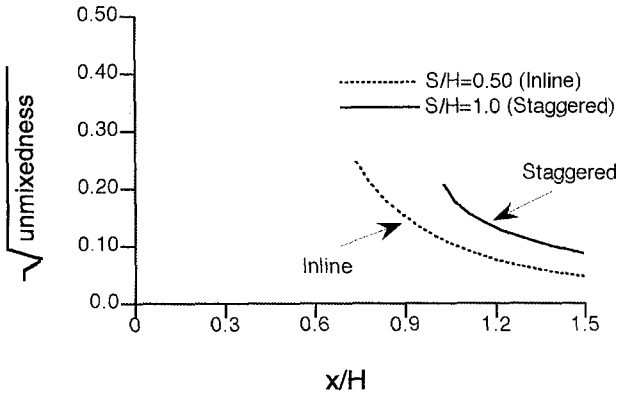

Figure 17: Effect of lateral arrangement on unmixedness at J = 16 (data from Bain et al. 1995b)

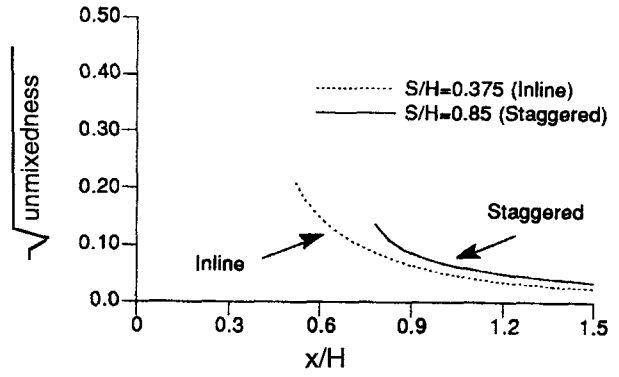

Figure 18: Effect of lateral arrangement on unmixedness at J = 36 (data from Bain et al. 1995b)

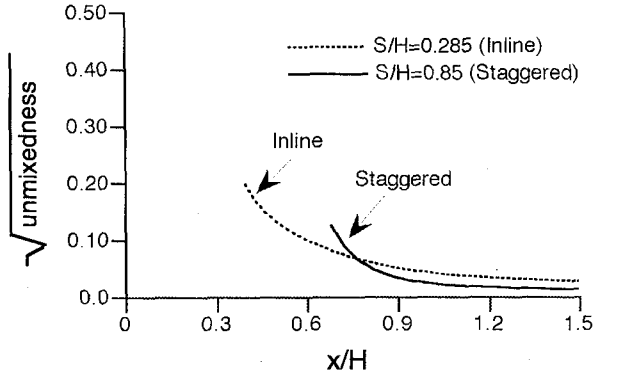

Figure 19: Effect of lateral arrangement on unmixedness at J = 64 (data from Bain et al. 1995b)

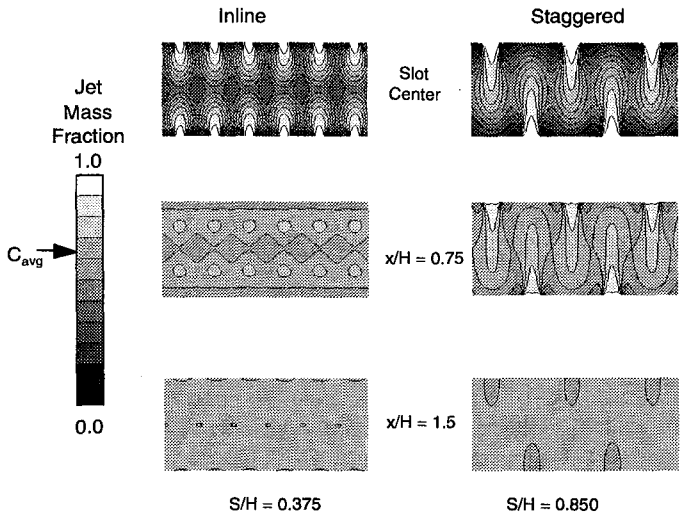

Figure 20: Effect of lateral arrangement on mixing; J = 36, MR = 2.0 (data from Bain et al. (1995b))

Vertical-transverse distributions for J = 36 are shown in Figure 20. This figure shows jet mass fraction concentrations at three downstream locations for optimum in-line and staggered configurations. It can be seen that although optimum in-line configuration offer better initial mixing, the staggered case seems to "catch up."

When experimental mixing tests are performed, only a limited number of configurations can be tested. Typically in-line arrangements are tested, followed by a lateral movement of one wall to create a staggered configuration. If an in-line configuration at a given J is optimized (upper left in Fig. 21), the corresponding staggered arrangement produced by laterally shifting one wall will produce nearly identical mixing as shown in upper right of Figure 21.

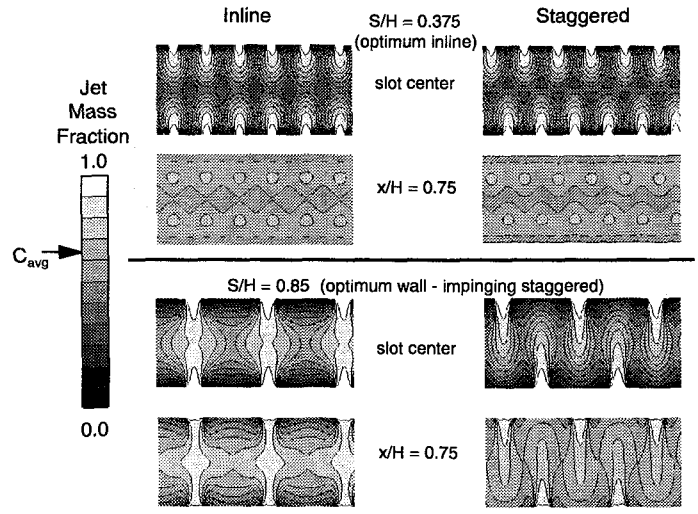

Figure 21: Comparison of inline and staggered slots at optimum S/H and J = 36, MR = 2.0 (data from Bain et al. (1995b))

The converse isn't true though: if a staggered arrangement is optimized (lower right in Fig. 21) at a given J, then the corresponding in-line case would produce inferior mixing (lower left of Fig. 21). Thus, optimized in-line configurations are more "tolerant" to alignment, and at low momentum-flux ratios are better mixers, so one would be inclined to choose them unless optimized staggered configurations are clearly better.

The relative insensitivity of optimized and underpenetrating in-line configurations to alignment is also shown experimentally in the results of Liscinsky et al. (1992) repeated in Figure 22. Note that one has the option of slanting the slots in the same (parallel) or opposite (crossed) direction on opposite sides of the duct, but this makes very little difference as seem in the Figure 22.

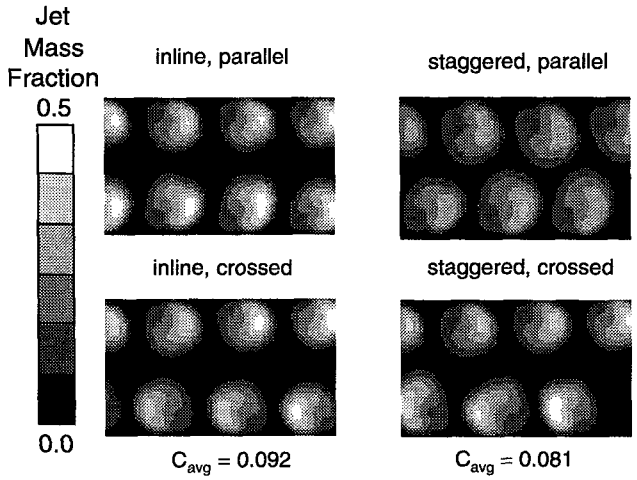

Figure 22: Concentration distributions of opposed slanted slots at J = 16, S/H = 0.5 and x/H = 0.33 (data from Liscinsky et al. (1992))

3.6 Effects of non-symmetric mass addition

Variation of orifice sizes on opposite walls. In practical confined mixing applications the flow may not be symmetric about a plane parallel to and midway between opposing walls, for example in an annulus. However most experimental and computational studies have focused on configurations that are symmetric, i.e. opposing jets are equal in area and momentum-flux ratio, J, and therefore mass addition is symmetric. Correlations that predict optimum mixing performance based on Eq. 4 and these data sets often assume symmetry and generally utilize duct height, H, as a non-dimensionalization parameter. Besides being convenient, H is important since jet penetration is key to mixing performance. But what if mass addition is non-symmetric ? What is the correct value for the equivalent height ?

The effect of non-symmetric mass addition is illustrated in Figure 23 comparing the jet mass fraction distribution at four downstream locations for tests with H/d = 2.67 on the top, and H/d = 4 on the bottom, both with S/H = 0.5. A grayscale is used to represent contours of jet mass fraction from 0 to 1.0 (pure mainstream fluid = black and pure jet fluid = white). In each of the tests the top orifice configuration was about twice the area of the bottom orifice configuration.

On the left, the opposing values of J were equal but the top and bottom mass flow were not equal due to the different orifice area. The distribution shows a minimum on the duct centerline (H/2), which is not surprising since the jet trajectories were optimized for H/4 penetration using Eq. 4. On the right side the opposing mass flows were equal but the values of J were unequal so as to obtain an equal mass balance through different sized orifices. The minimum in the concentration distribution is now nearer to the top wall (the lower J side).

The effective duct height, H_{eq}, is obvious for single side injection (H_{eq}=H), and for opposed rows of in-line orifices with symmetric flow and geometry (H_{eq}=(H/2)). It is not so obvious, however, for asymmetric conditions.

Two of the H_{eq} formulations from Liscinsky et al. (1996) are plotted on Figure 23 at the second downstream location. The solid line corresponds to the C formulation while the dashed line corresponds to a mass-flow ratio, MR, formulation.

The first of these formulation (solid line) is based on Eq. 4, where $C = (S/H)\sqrt{J}$:

$$[H_{eq}/H]_{C,top} = C_{top}/(C_{top} + C_{bottom}) \quad (5)$$

The other (dashed line) formulation is a mass-flow ratio balance:

$$[H_{eq}/H]_{MR,top} = MR_{top}/(MR_{top} + MR_{bottom}) \quad (6)$$

It follows that:

$$[H_{eq}/H]_{bottom} = 1 - [H_{eq}/H]_{top} \quad (7)$$

It appears that the better fit is obtained with the formulation based on C, i.e. the value of H_{eq} appears to depend on jet penetration which is determined by the product of S/H and the square root of J, rather than mass flow.

Variation of momentum-flux ratio on opposite walls. Similar results were obtained by varying opposing values of J with inline circular orifices with H/d = 8 spaced at S/H = 0.25 in Liscinsky et al. (1994). The effect of varying opposing J values is compared to results of an empirical model (Holdeman & Srinivasan, 1986) in Figure 24. In this experiment the orifice plate was held constant, H/d = 8, with S/H = 0.25, while the opposing J values were varied to maintain a mass-flow ratio (MR) of 0.325. This orifice configuration was found to be an optimal in-line configuration when opposing momentum-flux ratios were equal, and also an optimal configuration for one side injection at the same MR. The concentration distributions vary as expected, in that jet penetration is proportional to $\sqrt{J}$. Equivalent heights (from Eq. 5 & 6) are also shown on Figure 24 (because of the way the experiment was performed Eq. 5 & 6 give the same results). Although S/H was not varied in either of these investigations, the value of H_{eq} appears to be independent of orifice diameter.

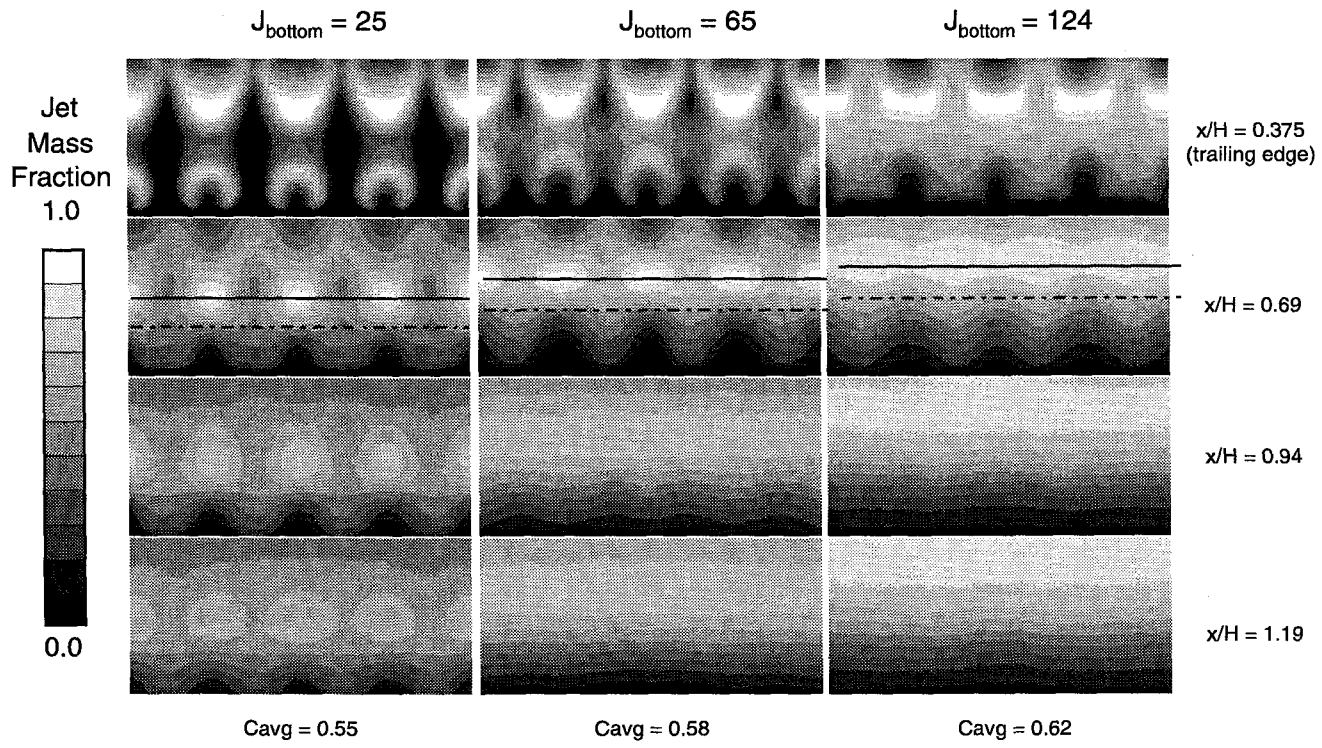

Figure 23: Effect of non-symmetric mass addition; J_{top} = 25, H/d_{top} = 2.67, H/d_{bottom} = 4.0, S/H = 0.5 (data from Liscinsky et al. (1996))

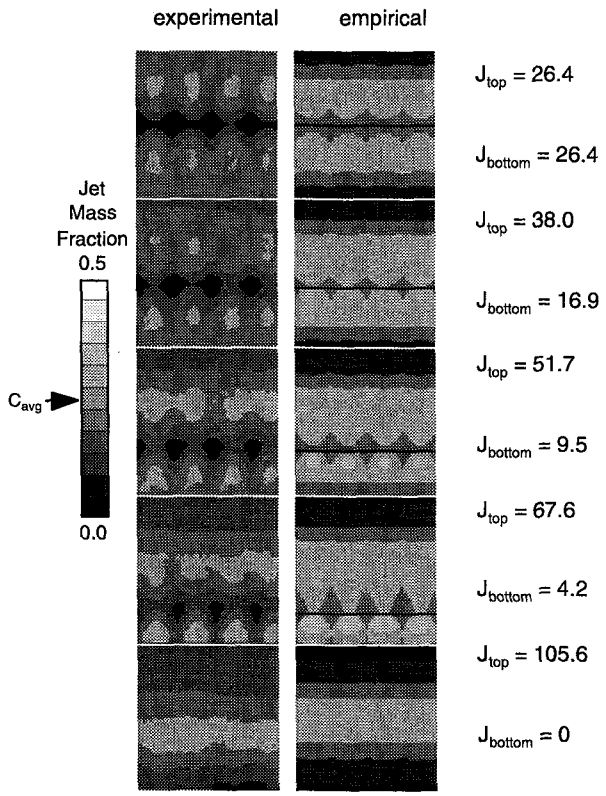

Figure 24: Comparison of experimental and empirical results for inline round orifices when opposing J values are unequal (S/H = 0.25 and x/H = 0.5) (data from Liscinsky et al. (1994))

3.7 Effect of orifice blockage

The inverse relation between $\sqrt{J}$ and S/H given in Eq. 4 has been shown to apply (e.g. Bain et al., 1994) when extended to typical RQL conditions of MR > 2 and S/d < 2. However at those conditions the proportionality constant C has been found, both experimentally (Liscinsky et al., 1993) and computationally (Bain et al., 1993 & 1994) to be ~2.5 rather than the expected value of ~1.25. Thus C appeared to be a function of something, and orifice blockage (B) was a possibility. In this summary, as in all previous studies in this program, blockage is defined as the ratio of the transverse projection of the orifice to the spacing between corresponding locations of adjacent orifices - note that B = 1/(S/d) for circular holes.

To determine whether C was a discernible function of orifice blockage, a set of rectangular orifice configurations were designed and tested. A schematic of the configurations is shown in Table 1 in Liscinsky, et al. (1994). A J of 36 was chosen, and the mass-flow ratio (MR) and orifice spacing (S/H) were maintained constant at MR = 2 and S/H = 0.425 for all, while the orifice blockages (B) varied substantially. The configurations examined were based on a numerical study by Bain et al. (1994), in which orifice aspect ratio and shape were found to have little effect on the mixing performance of in-line configurations when a value of 2.55 was used for C in Eq. 4.

Average jet mass fraction distributions, perpendicular to the mainstream flow direction, are shown in Figure 28 for blockages (B) varying from 0.59 to 0.89. Five downstream planes are shown from the trailing edge of these orifices (at the top) to a distance equal to one-half duct height

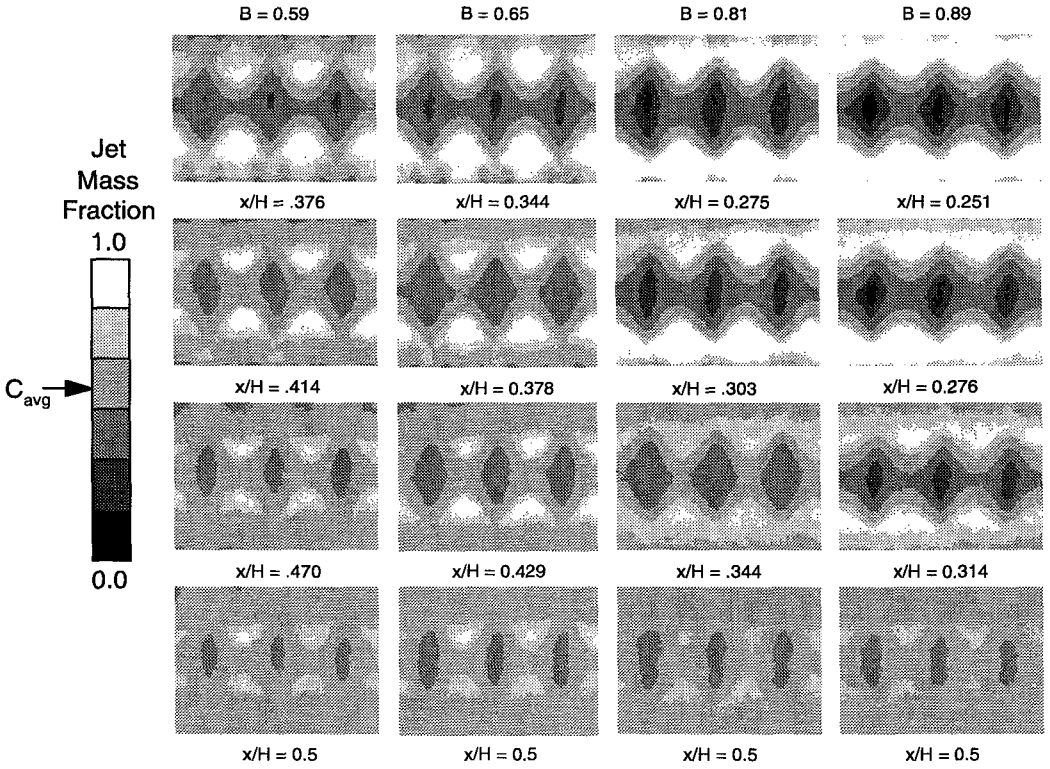

Figure 25: Effect of Orifice Blockage on Opposed Inline Rectangular Orifices; MR = 2.0, S/H = 0.425, J = 48 (data from Liscinsky et al. (1994))

downstream (at the bottom). The corresponding unmixedness curves are shown in Figure 26. Obviously, the mixing from all these configurations is very similar, although the distance between orifices is only about 13% of the orifice width for the largest blockage shown.

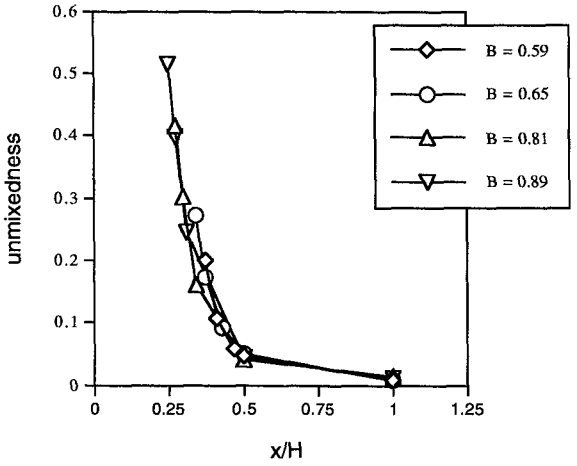

Figure 26: Effect of orifice blockage on spatial unmixedness; MR = 2.0, S/H = 0.425, and J = 48 (data from Liscinsky et al. (1994))

3.8 Variation of mass-flow ratio

The effect of mass-flow ratio is shown in the centerplane distributions in Figure 27 from Bain et al. (1994). The corresponding vertical-transverse planes at x/H = 0.5 are shown in Figure 28. These are all at the "optimum" spacing for each configuration. Clearly the penetration is about the same for these. Note though, that for the MR = 2 case the jets are still entering the flowfield at this axial location.

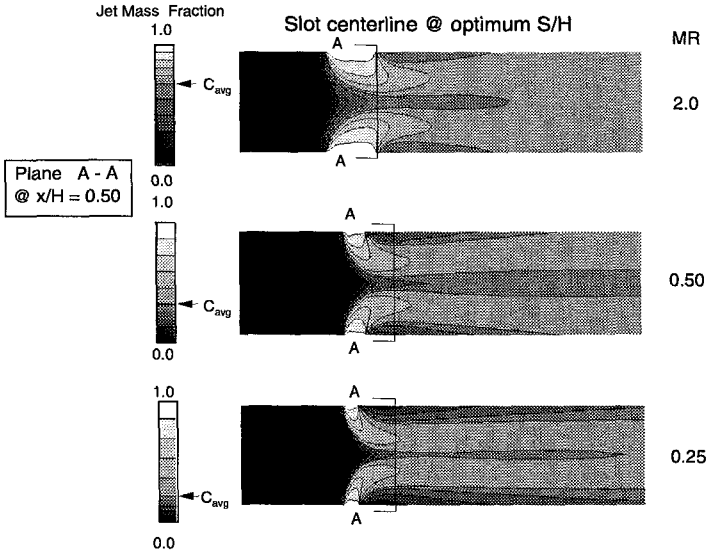

Figure 27: Effect of jet-to-mainstream mass flow variation on jet penetration at optimum S/H and J = 36, L/W = 4 (data from Bain et al. (1994))

The unmixedness curves for these configurations are given in Figure 29. Note that the optimum S/H is 0.375 for MR = 2, whereas the optimum is only S/H = 0.25 for MR = 0.25. This variation suggests that there may be a significant effect of MR on C. Although for x/H > 0.7 the MR = 2 case exhibits slightly lower unmixedness than the others, it and the MR = 0.5 case show higher values between x/H = 0.3 and x/H = 0.7 probably due to their larger size.

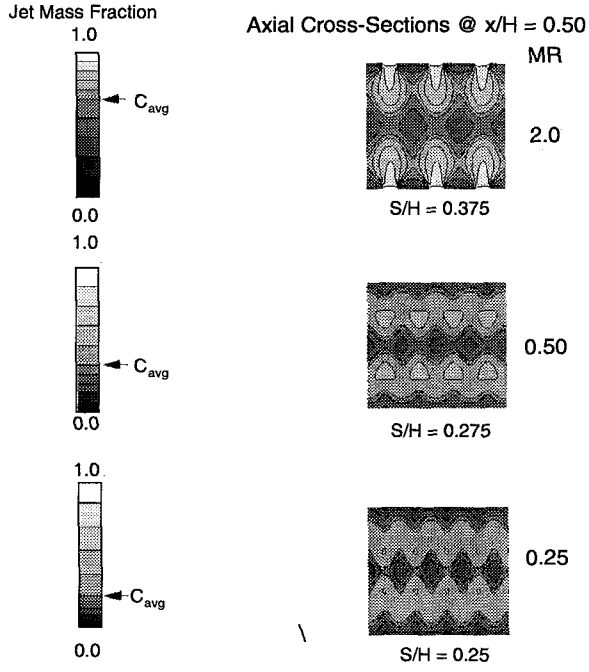

Figure 28: Effect of jet-to-mainstream mass flow ratio on jet penetration at J = 36, MR = 2.0 (data from Bain et al. (1994))

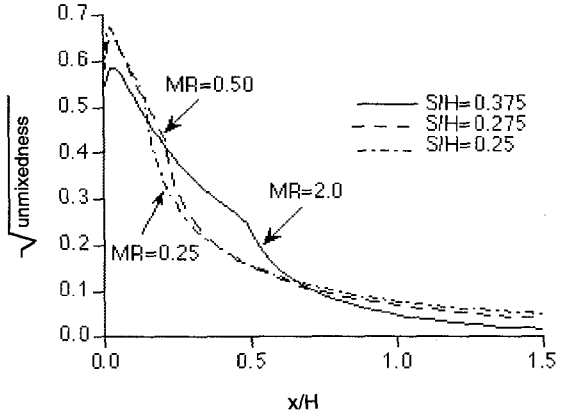

Figure 29: Effect of jet-to-mainstream mass flow ratio on unmixedness at optimum S/H; orifice aspect ratio = 4, J = 36 (data from Bain et al. (1994))

4. Design Procedure

These results suggest that for a given momentum-flux ratio and downstream distance, combustor design procedure should first identify the momentum-flux ratio, effective orifice area, and the orifice spacing required to obtain the desired penetration and profile shape. The orifice size would then be chosen to provide the required jet-to-mainstream mass-flow ratio. Some adjustments, including non-circular orifices or multiple rows, may be needed to arrive at the final design because jet penetration varies slightly with orifice size and shape, and other parameters such as the combustor pressure loss and the ratio of the orifice spacing to diameter must be monitored to insure that the suggested configuration is physically realistic. Also it should be noted that since jet penetration often varies with axial distance, one must consider both 'what' and 'where' in the optimization.

Based on these results, the suggested procedure is, given mass-flow ratio, pressure drop, and channel height:

1) Calculate momentum-flux ratio (J)
2) Identify needed effective orifice area
3) Choose desired orifice shape
4) Select number of orifices for optimum penetration
5) Calculate individual orifice size
6) Determine blockage, fit, etc.
7) Iterate to solution

Summary of Results

A) Several results from recent studies are consistent with results from previous investigations. These include:

1) Variations in momentum-flux ratio and orifice spacing have a significant effect on the flow distribution.
2) Optimum configurations may depend on given momentum-flux ratio.
3) The optimum orifice spacing is inversely proportional to the square root of the momentum-flux ratio.
4) Optimum spacing may vary with orifice shape.
5) Similar jet penetration can be obtained, largely independent of orifice size and shape, when orifice spacing (S/H) is inversely proportional to the square-root of the momentum-flux ratio (J). Note that although orifice configurations can be optimized for any J, a shorter downstream distance is required for equivalent mixing if J is large and/or the orifice spacing is small.
6) The penetration of slanted slots is less than for equal-area circular holes.
7) For orifices that are symmetric with respect to the main flow direction, the effects of shape are significant only in the region near the injection plane. Beyond x/H = 1, scalar distributions were similar to those observed from equally spaced equal-area circular orifices.
8) Planar average mixing often increases monotonically with momentum-flux ratio (J). Since overpenetration cases are usually not desirable, this emphasizes the importance of perusing both the distributions and planar averages before identifying an optimum configuration.

B) Conclusions that are unique to the current investigations include:

1) Although the current studies confirmed the inverse proportionality between orifice spacing (S/H) and the square root of the momentum-flux ratio (J), the optimum constant of proportionality for rectangular ducts at MR > 1.0 appears to be about twice that reported by Holdeman (1993).
2) For opposed rows of round holes with centerlines in-line, mixing was similar for blockages from 0.5 to 0.90.
3) In-line configurations have better initial mixing than staggered configurations at their respective optimums.
4) For downstream mixing (x/H>1.5), optimum in-line configurations appear to be better mixers than staggered ones for low Js (i.e. 16), but the opposite may be true for high momentum-flux ratios (i.e. J>64).
5) The vortex pattern formed by optimum in-line configurations appears to be quite different than that from optimum staggered configurations. The latter may destabilize more quickly than optimum in-line jets, so properly spaced staggered configurations may augment downstream mixing.
6) Different orifice shapes may not have the same optimum spacing for a given J, so comparison should be obtained from optimum configurations.
7) Orifice aspect ratio had little effect on jet penetration and mixing.
8) For non-symmetric mass addition from opposite sides of the duct, an effective duct height based on the momentum-flux ratio and the orifice spacing can be used to determine the optimum mixer for opposed in-line injection.

Acknowledgments

The authors would like to acknowledge the contributions of the following: R.P. Lohmann, Pratt & Whitney Aircraft; H.C. Mongia, GE Aircraft Engines (formerly with Allison); V.L. Oechsle, Allison Advanced Development Company; G.S. Samuelsen, University of California, Irvine (UCI); C.E. Smith, CFD Research Corporation; W.A. Sowa, United Technologies Research Center (UTRC) (formerly at UCI); B. True, UTRC; A. Vranos, University of Connecticut (formerly with UTRC), and M. Winter, UTRC.

References

Bain, D. B., Smith, C. E., and Holdeman, J. D. (1992). CFD Mixing Analysis of Jets Injected From Straight and Slanted Slots Into a Confined Crossflow in Rectangular Ducts. AIAA Paper 92-3087 (also NASA TM 105699).

Bain, D. B., Smith, C. E., and Holdeman, J. D. (1994). CFD Assessment of Orifice Aspect Ratio and Mass Flow Ratio on Jet Mixing in Rectangular Ducts. AIAA Paper 94-0218 (also NASA TM 106434).

Bain, D. B., Smith, C. E., and Holdeman, J. D. (1995a). Jet Mixing and Emission Characteristics of Transverse Jets in Annular and Cylindrical Confined Crossflow. AIAA Paper 95-2995 (also NASA TM 106976).

Bain, D. B., Smith, C.E., and Holdeman, J. D. (1995b). Mixing Analysis of Axially Opposed Rows of Jets Injected into Confined Crossflow. *Journal of Propulsion and Power*, Vol.11, No.5, pp.885-893, Sep-Oct. (see also AIAA Paper 93-2044 & NASA TM 106179).

Bain, D.B., Smith, C.E., Liscinsky, D.S., and Holdeman, J.D. (1996). Flow Coupling Effects in Jet-in-Crossflow Flowfields. AIAA Paper 96-2762 (also NASA TM 107257).

Blomeyer, Malte M., Krautkremer, Bernd H., and Hennecke, Dietmar K. (1996). Optimum Mixing for a Two-sided Injection from Opposed Rows of Staggered Jets in a Confined Crossflow. ASME Paper 96-GT-483, June.

Chiu, S., Roth, K.R., Margason, R.J., and Tso, J. (1993). A Numerical Investigation of a Subsonic Jet in a Crossflow. AIAA Paper 93-0870.

Chiu, Stephen H., Roth, Karlin R., Margason, Richard J., and Tso, Jin (1993). A Numerical Investigation of a Subsonic Jet in a Crossflow. Computational and Experimental Assessment of Jets in Cross Flow, AGARD Conference Proceedings 534..

Crocker, D. Scott and Smith, Clifford E. (1993). Numerical Investigation of Enhanced Dilution Zone Mixing in a Reverse Flow Gas Turbine Combustor. ASME Paper 93-GT-129.

Crocker, D. Scott and Smith, Clifford E. (1994). Numerical Investigation of Angled Dilution Jets in Reverse Flow Gas Turbine Combustors. AIAA Paper 94-2771.

Crocker, D. Scott, Smith, Clifford E., and Myers, Geoff D. (1994). Pattern Factor Reduction in a Reverse Flow Gas Turbine Combustor Using Angled Dilution Jets. ASME Paper 94-GT-406.

Doerr, Th. and Henneke, D.K. (1993). The Mixing Process in the Quenching Zone of the Rich-Lean Combustion Concept. AGARD-PEP 81st Symposium of Fuels and Combustion Technology for Advanced Aircraft Engines.

Doerr, Th., Blomeyer, M., and Henneke, D.K. (1995a). Optimization of Multiple Jets Mixing with a Confined Crossflow. ASME Paper 95-GT-313.

Doerr, Th., Blomeyer, M., and Henneke, D.M. (1995b). Experimental Investigation of Optimum Jet Mixing Configurations for RQL-Combustors, 12th ISABE, Melborne Aus.

Everson, R., Manin, D., Sirovich, L., and Winter, M. (1995). Quantification of Mixing and Mixing Rate from Experimental Observations. Accepted for publication in AIAA Journal (also AIAA Paper 95-0169).

Hatch, M.S, Sowa, W.A., Samuelsen, G.S., and Holdeman, J.D. (1995). Geometry and Flow Influences on Jet Mixing in a Cylindrical Duct. *Journal of Propulsion and Power*, Vol.11, No.3, pp393-402, May-June (see also "Jet Mixing Into a Heated Cross Flow in a Cylindrical Duct: Influence of Geometry and Flow Variations", AIAA-92-9773 & NASA TM 105390).

Holdeman, James D., Walker, R.E., and Kors, D.L. (1973). Mixing of Multiple Dilution Jets With a Hot Primary Airstream for Gas Turbine Combustors. AIAA Paper 73-1249 (also NASA TM X-71426).

Holdeman, J.D. (1993). Mixing of Multiple Jets With a Subsonic Crossflow. *Prog. Energy Combust. Sci.*, Vol.19, pp.31-70 (see also AIAA-91-2458 & NASA TM 104412).

Holdeman, James D., Liscinsky, David S., Oechsle, Victor L., Samuelsen, G.Scott, and Smith, Clifford E. (1996). Mixing of Multiple Jets With a Confined Subsonic Crossflow in a Cylindrical Duct. Accepted for publication in *Journal of Engineering for Gas Turbines and Power* (also ASME Paper 96-GT-482 and NASA TM 107185), June.

Liscinsky, D. S., True, B., Vranos, A., and Holdeman, J. D. (1992). Experimental Study of Crossflow Jet Mixing in a Rectangular Duct. AIAA Paper 92-3090, (also NASA TM 105694.

Liscinsky, D.S., Vranos, A., and Lohmann, R.P. (1993). Experimental Study of Cross-Stream Mixing in Cylindrical and Rectangular Ducts. NASA CR 187141.

Liscinsky, D.S., True, B., and Holdeman, J.D. (1993). Experimental Investigation of Crossflow Jet Mixing in a Rectangular Duct. AIAA Paper 93-3090 (also NASA TM 106152).

Liscinsky, D.S., True, B., and Holdeman, J.D. (1994). Mixing Chracteristics of Directly Opposed Rows of Jets Injected Normal to a Crossflow in a Rectangular Duct. AIAA Paper 94-0217 (also NASA TM 106477).

Liscinsky, D.S., True, B., and Holdeman, J.D. (1995). Effect of Initial Conditions on a Single Jet in Crossflow. AIAA Paper 95-2998 (also NASA TM 107002).

Liscinsky, D.S., True, B., and Holdeman, J.D. (1996a). Crossflow Mixing of Noncircular Jets. *Journal of Propulsion and Power*, Vol.12, No.1 (see also AIAA Paper 95-0732 and NASA TM 106865).
Liscinsky, D.S., True, B., and Holdeman, J.D. (1996b). Effect of Inlet Flow Conditions of Crossflow Jet Mixing. AIAA Paper 96-2881 (also NASA TM 107258).

Lozano, A., Smith, S.H., Mungal, M.G., and Hanson, R.K. (1991). Concentration Measurements in a Transverse Jet by Planar Laser-Induced Florescence of Acetone. *AIAA Journal* Vol.32, No. 1, pp.218-221.

Lozano, A., Yip, B., and Hanson. R. K. (1992). Acetone: A Tracer for Concentration Measurements in Gaseous Flows by Planar Laser-Induced Fluorescence. *Experiments in Fluids* Vol.13, pp. 369-376.

Margason, Richard J. (1993). Fifty Years of Jet in Cross Flow Research Computational and Experimental Assessment of Jets in Cross Flow, AGARD Conference Proceedings 534.

Margason, Richard J. and Tso, Jin (1993). Jet to Freestream Velocity Ratio Computations for a Jet in a Crossflow. AIAA Paper 93-4860.

Mungal, M.G., Lozano, A., and van Cruyningen, I. (1992). Large-Scale Dynamics in High Reynolds Number Jets and Jet Flames. *Experiments in Fluids*, Vol. 12, No. pp.141-150.

Nikjooy, M., Mongia, H.C., Sullivan, J.P., and Murthy, S.N.B. (1993). Flow Interaction Experiment - Aerothermal Modeling Phase II, Vols. I & II. NASA CR 189192.

Oechsle, V.L., Mongia, H.C., and Holdeman, J.D. (1992). A Parametric Numerical Study of Mixing in a Cylindrical Duct. AIAA Paper 92-3088, 1992 (also NASA TM 105695).

Smith, S.H., Lozano, A., Mungal, M.G., and Hanson, R.K. (1992). Scalar Mixing in the Subsonic Jet in Crossflow. AGARD Computational and Experimental Assessment of Jets in Cross Flow.

Winter, M., Barber, T.J., Everson, R., and Sirovich. L. (1992). Eigenfunction Analysis of Turbulent Mixing Phenomena. *AIAA Journal*, Vol.30, No.7.

Wittig, S.L.K., Elbahar, O.M.F., and Noll, B.E. (1984). Temperature Profile Development in Turbulent Mixing of Coolant Jets with a Confined Hot Crossflow. *Journal of Engineering for Gas Turbines and Power*, Vol.106, pp. 193ff.

REPORT DOCUMENTATION PAGE

Form Approved
OMB No. 0704-0188

1. AGENCY USE ONLY (*Leave blank*)	2. REPORT DATE	3. REPORT TYPE AND DATES COVERED
	May 1997	Technical Memorandum

4. TITLE AND SUBTITLE

Mixing of Multiple Jets With a Confined Subsonic Crossflow
Part II—Opposed Rows of Orifices in Rectangular Ducts

5. FUNDING NUMBERS

WU–537–02–20–00

6. AUTHOR(S)

James D. Holdeman, David S. Liscinsky, and Daniel B. Bain

7. PERFORMING ORGANIZATION NAME(S) AND ADDRESS(ES)

National Aeronautics and Space Administration
Lewis Research Center
Cleveland, Ohio 44135–3191

8. PERFORMING ORGANIZATION REPORT NUMBER

E–10747

9. SPONSORING/MONITORING AGENCY NAME(S) AND ADDRESS(ES)

National Aeronautics and Space Administration
Washington, DC 20546–0001

10. SPONSORING/MONITORING AGENCY REPORT NUMBER

NASA TM–107461
ASME–97–GT–439

11. SUPPLEMENTARY NOTES

Prepared for the 42nd Gas Turbine and Aeroengine Congress sponsored by the International Gas Turbine Institute of the American Society of Mechanical Engineers, Orlando, Florida, June 2–5, 1997. James D. Holdeman, NASA Lewis Research Center; David S. Liscinsky, United Technologies Research Center, East Hartford, Connecticut 06108; and Daniel B. Bain, CFD Research Corporation, Huntsville, Alabama 35805. Responsible person, James D. Holdeman, organization code 5830, (216) 433–5846.

12a. DISTRIBUTION/AVAILABILITY STATEMENT

Unclassified - Unlimited
Subject Category: 07

Available electronically at http://gltrs.grc.nasa.gov/GLTRS
This publication is available from the NASA Center for AeroSpace Information, (301) 621–0390.

12b. DISTRIBUTION CODE

13. ABSTRACT ***(Maximum 200 words)***

This paper summarizes experimental and computational results on the mixing of opposed rows of jets with a confined subsonic crossflow in rectangular ducts. The studies from which these results were excerpted investigated flow and geometric variations typical of the complex 3-D flowfield in the combustion chambers in gas turbine engines. The principal observation was that the momentum-flux ratio, J, and the orifice spacing, S/H, were the most significant flow and geometric variables. Jet penetration was critical, and penetration decreased as either momentum-flux ratio or orifice spacing decreased. It also appeared that jet penetration remained similar with variations in orifice size, shape, spacing, and momentum-flux ratio when the orifice spacing was inversely proportional to the square-root of the momentum-flux ratio. It was also seen that planar averages must be considered in context with the distributions. Note also that the massflow ratios and the orifices investigated were often very large (jet-to-mainstream mass-flow ratio >1 and the ratio of orifices-area-to-mainstream-cross-sectional-area up to 0.5 respectively), and the axial planes of interest were often just downstream of the orifice trailing edge. Three-dimensional flow was a key part of efficient mixing and was observed for all configurations.

14. SUBJECT TERMS

Dilution; Jet mixing; Rectangular duct; Gas turbine combustion chamber

15. NUMBER OF PAGES

17

16. PRICE CODE

A03

17. SECURITY CLASSIFICATION OF REPORT	18. SECURITY CLASSIFICATION OF THIS PAGE	19. SECURITY CLASSIFICATION OF ABSTRACT	20. LIMITATION OF ABSTRACT
Unclassified	Unclassified	Unclassified	